IRIS AperTO

UNIVERSITÀ DEGLI STUDI DI TORINO

AperTO - Archivio Istituzionale Open Access dell'Università di Torino

Fate of antibacterial spiramycin in river waters

This is the author's manuscript

Original Citation:

Availability:

This version is available http://hdl.handle.net/2318/77046 since

Published version:

DOI:10.1007/s00216-009-3318-3

Terms of use:

Open Access

Anyone can freely access the full text of works made available as "Open Access". Works made available under a Creative Commons license can be used according to the terms and conditions of said license. Use of all other works requires consent of the right holder (author or publisher) if not exempted from copyright protection by the applicable law.

(Article begins on next page)

13 December 2025

UNIVERSITÀ DEGLI STUDI DI TORINO

This is an author version of the contribution published on:
Questa è la versione dell'autore dell'opera:
P. Calza, S. Marchisio, C. Medana, C. Baiocchi. Anal Bioanal Chem (2010) 396:1539–1550
DOI 10.1007/s00216-009-3318-3

The definitive version is available at:
La versione definitiva è disponibile alla URL:
http://link.springer.com/article/10.1007%2Fs00216-009-3318-3

Fate of the Antibacterial Spiramycin in River Waters

P. Calza *, S. Marchisio, C. Medana, C. Baiocchi

Department of Analytical Chemistry and NIS Centre of Excellence, University of Turin, via P. Giuria 5, 10125 Torino, Italy

*corresponding author. Phone: +390116707626; fax: +390116707615; e-mail: paola.calza@unito.it

Abstract

Spiramycin, a widely used veterinary macrolide antibiotic, was found at traceable levels (ng/L range) in Po River water (N-Italy). The aqueous environmental fate of this antibiotic compound was studied through drug decomposition, the identification of the main and secondary transformation products (TPs), assessment of mineralization, and the investigation of drug TPs toxicity. Initially, laboratory experiments were performed, with the aim to simulate the antibacterial transformation processes followed in aquatic systems. The TPs were identified through the employment of LC-MS technique. Under illumination, spiramycin was degraded rapidly and transformed into numerous organic (intermediate) compounds, of which eleven could be identified, formed through five initial transformation routes. These laboratory simulation experiments were verified in field to check the mechanism previously supposed. Po River water was sampled and analysed (by LC-HRMS) at eight sampling points. Among the previously identified TPs, five of them were also found in the river water. Three of them seem to be formed through a direct photolysis process, while the other two are formed through indirect photolysis processes mediated by natural photo sensitizers. The transformation occurring in the aquatic system involved hydroxylation, demethylation and the detachment of forosamine or mycarose sugars. Toxicity assays using *Vibrio fischeri* proved that even if spiramycin did not exhibit toxicity, its transformation proceeded through the formation of toxic products.

Keywords: spiramycin, antibiotics, photochemistry, transformation products, river water, toxicity

1. Introduction

Since 1990's an increasing attention has been focused on the introduction of pharmaceutical agents (PhACs) in the environment [1-3]. Human and veterinary applications are the main sources of PhACs in the environment, that are introduced through excretion and the subsequent transport in sewage. Conventional sewage treatments are not able to completely remove these pollutants and their metabolic products [4] and, as a result, pharmaceutical contaminants are introduced into the aquatic environment. In addition, due to their polar nature, several pharmaceuticals are not significantly adsorbed in the subsoil and during recharge and from landfill may leach into groundwater. Their concentrations have been assessed in many countries at parts per-billion (ppb) and parts-per-trillion (ppt) in wastewater, surface water, as well as drinking water [5-6]. Although these levels are much lower than those used in medical applications, the related potential toxic effects are still poorly known and cannot be discarded. The concentration of these residues in the aquatic environment is too low to pose a very acute risk, but it is unknown whether other receptors in non-target organisms are susceptible to individual residues, or if the combination of drugs sharing a common mechanism of action could exhibit synergistic effects [7]. The elimination of antibacterials mainly occurs as parent compounds and then considerable quantities of active drugs are discharged in the environment [8]. Degradation products may also promote microbial resistance, above all if the active part of the molecule remains unmodified. Consequently, monitoring not only drug degradation but also drug metabolites is of increasing relevance in evaluating their environmental impact.

Macrolide antibiotics are molecules with a central lactone ring bearing 12 or 16 atoms to which several amino and/or neutral sugars are bound, widely diffused [9] and particularly adopted for veterinary practise [10]. The more suitable techniques for their determination are LC/MS and LC/MS/MS [11-15]. In our study, we have focused on spiramycin, a macrolide antibacterial agent found at trace level in Po River waters [16-18]. It has a lactone ring bearing 16 carbon atoms and three sugar molecules: a molecule of mycarose, mycaminose and forosamine [19] (see Figure 1). It is a mixture of spiramycin I (over 85%) together with its 3-acetyl (Spiramycin II) and 3-propanoyl- (Spiramycin III) esters [20]. Spiramycin is active against Gram-positive and some Gram-negative bacteria and is mostly used for veterinary purposes; for such, the available studies deals on its determination in animal tissue [21] and on metabolism in animal liver [22].

The goal of this study is to enlighten the fate of this drug in the aquatic environment. This aim could be fulfilled through a combined evaluation of different aspects: 1) drug decomposition; 2) characterization of the transformation products; 3) assessment of mineralization and 3) evaluation

of the TPs toxicity. Identification of TPs was done by HPLC/MS, ESI positive mode A bacterial assay was carried out based on the bioluminescence reduction of the marine bacterium *Vibrio fischeri.*

Firstly, laboratory simulations were performed. For such, a photocatalytic process using titanium dioxide was employed as a model-system. Heterogeneous photocatalysis represents an example of advanced oxidation processes (AOPs) capable of achieving a complete oxidation of organic and inorganic species, including also pharmaceutical substances [23-27]. Moreover, it is known that the photocatalytic process can be used to artificially produce degradation compounds similar to those formed in oxido/reductive metabolic and environmental pathways [28].

Laboratory experiments were performed in sterilized or river water spiked with spiramycin under simulated solar light, in the presence or absence of a photocatalyst. Afterwards, spiramycin and its identified TPs were monitored in eight samples collected from the Po River.

2. Experimental Section

2.1. Material and Reagents

Spiramycin (purity > 90%, solubility in water > 20 mg L^{-1} [29]) was purchased from Aldrich. HPLC grade acetonitrile (BDH) was filtered through a 0.45 μm filter before use. Formic acid reagent grade was purchased from Carlo Erba. Experiments were carried out using spiramycin in water (18 mg L^{-1}) and TiO_2 Degussa P25 100 mg L^{-1} as the photocatalyst.

2.2. Irradiation Procedures

The irradiation experiments were carried out in Pyrex glass cells. The illumination was performed using a 1500 watt Xenon lamp (CO.FO.MEGRA, Milan, Italy) equipped with a 340 nm cut-off filter simulating AM1 solar light. The temperature reached during the irradiation was 38 ± 2°C.

2.3. Analytical Procedures

2.3.1. Liquid Chromatography

The chromatographic separations of the samples prepared during laboratory simulations were run on two HPLC/MS instruments: (1) a Surveyor HPLC equipped with a MSQ mass spectrometer (Thermo Fisher) and (2) a Ultimate 3000 HPLC (Dionex) a LTQ Orbitrap mass spectrometer

(ThermoFisher, Rodano, Italy), both equipped with an atmospheric pressure interface and an ESI ion source was used. In case (1), analysis HPLC were run using a RP18 Merck Lichrosphere column (250 × 4 mm, 5 μm particle size). Injection volume was 20 μL and flow rate 1 mL/min. Gradient mobile phase composition was adopted: 100/0 to 50/50 in 14 min ammonium acetate 0.05% / acetonitrile. The LC column effluent was delivered into the ion source using nitrogen as both sheath and auxiliary gas. The heated capillary value was maintained at 300 °C. The acquisition method used was previously optimized in the tuning sections for the parent compound (capillary, magnetic lenses and collimating octapoles voltages) in order to achieve the maximum of sensitivity. The tuning parameters adopted for ESI source have been the following: capillary voltage 2.5 V, RF Lens Bios 0.3 V, ion energy 1V. Mass spectra were collected in full scan positive mode in the range 50-900 *m/z*.

In case (2), samples were analyzed using a RP C18 column (Phenomenex Luna 150 × 2.1 mm, 3 μm particle size). Gradient mobile phase composition was adopted: 95/5 to 25/75 in 56 min 0.05% formic acid / acetonitrile. An ESI ion source was used. The tuning parameters adopted for the ESI source were: capillary voltage 37.00 V, tube lens 65 V. The source voltage was set to 3.5 kV. The heated capillary temperature was maintained at 275°C. Mass accuracy of recorded ions (vs calculated) was ± 2 ppm (with internal calibration).

2.3.2. Ion Chromatography

A Dionex instrument was employed equipped with a conductimetric detector. Determination of ammonium ions was achieved using a CS12A column and 25 mM metansulphonic acid as eluant, at a flow rate of 1 mL/min. In these conditions the retention time for ammonium ion was 4.7 min. The anions were analyzed using an AS9HC anionic column, 9 mM K_2CO_3 as eluant and a flow rate of 1 mL/min. In these experimental conditions the retention time of nitrate ions was 13.98 min.

2.3.3. Total Organic Carbon Analyzer

Total organic carbon (TOC) and not purgeable organic carbon (nPOC) were measured on filtered suspensions using a Shimadzu TOC-5000 analyzer (catalytic oxidation on Pt at 680 °C). The calibration was performed using standards of potassium phthalate.

2.3.4. Toxicity Measurements

The toxicity of an unirradiated spiramycin solution and of aqueous samples collected at different irradiation times, was examined by Microtox Model 500 Toxicity Analyzer. Toxicity was

evaluated by monitoring changes in the natural emission of the luminescent bacteria *Vibrio fischeri* when challenged with toxic compounds. Freeze-dried bacteria, reconstitution solution, diluent (2% NaCl) and an adjustment solution (non-toxic 22% sodium chloride) were obtained from Azur. Samples were tested in medium containing 2% sodium chloride, in five dilutions and luminescence was recorded after 5 and 15 min of incubation at 15 ^{o}C. Inhibition of the luminescence, compared with a toxic-free control to give the percentage of inhibition, was calculated following the established protocol using the Microtox calculation program.

2.4. Samples Treatment

Eight Po river samples were collected and concentrated by solid phase extraction (SPE) using Strata X (Phenomenex) cartridges. 200 mL of the water sample is added with 200 µL isoxsuprine (1 mg/L) as internal standard. Eluition was done with 2 mL CH_3OH, 2 ml NH_3 (2 % in CH_3OH). Eluted solution is dried under nitrogen flux and then added with 200 µL 0.05% formic acid and analyzed.

3. Results and Discussion

3.1. Spiramycin MS^n analysis

Spiramycin MS^n fragmentations study was done by employing a MSQ and a LTQ-Orbitrap analyzer. In both cases, the same peculiar losses were shown and the pathways were carefully considered in identifying the unknown compounds formed during the drug photoinduced degradation. At high cone voltage in MSQ analyzer, spiramycin ($[M+H]^+$ 843) produced the ions at *m/z* 699 and *m/z* 540. These product ions were also formed in MS^2 spectrum obtained from LTQ-Orbitrap analyzer, together with two additional product ions, all involving the detachment of the sugar moieties:

1) a product ion at *m/z* 699.4407 from the protonated molecular ion (*m/z* 843.5210), due to the loss of mycarose;

2) a product ion having *m/z* 684.3934 (loss of forosamine);

3) a fragment at *m/z* 540.3147 (combined elimination of forosamine and mycarose);

4) a product ion at *m/z* 522.3043 (concerted loss of forosamine, mycarose and a water molecule).

These ions were the precursors for the other ions summarized in Table 1 and should be linked through the fragmentation pathway proposed in Scheme 1.

Among them, particularly useful for the structural attributions of the compounds presented below were:

(1) the product ion at *m/z* 349.1923 formed from the MS^2 ion at *m/z* 540.3147 through the mycaminose detachment;
(2) a product ion at *m/z* 558.3132 formed from the neospiramycin through the forosamine detachment and;
(3) the production of *m/z* 490.2675 from the MS^2 ion at *m/z* 522.3043 through a methanol loss.

3.2. Spiramycin Degradation and Mineralization

The transformation of spiramycin (15 mgL^{-1}) was investigated:

1) in the dark, in sterilized or river water;
2) upon illumination, in sterilized or river water;
3) upon illumination in sterilized water added with TiO_2.

Analyses were run by HPLC/MS in positive ESI mode. The profiles as a function of the irradiation time are shown in Figure 2a. Dark experiments at 25 ± 2 °C showed that, in sterilized water, no degradation occurred. Hence, thermal hydrolysis can be neglected. Conversely, in Po river water biotic processes promoted the spiramycin disappearance ($t_{1/2}$ 260 h).

Upon light exposure, the complete disappearance of the drug occurred through a pseudo-first order decay. In sterilized water, $t_{1/2}$ was 48 h, further reduced to 25 h in river water. Hence, even if biotic degradation contributed to the spiramycin disappearance, aqueous photolysis was rapid and will be the main route of degradation in aquatic systems exposed to sunlight. Furthermore, both direct and indirect photolysis processes took part to the spiramycin degradation. When titanium dioxide was added, the complete degradation easily occurred ($t_{1/2}$ 3 min, see inset in Figure 2a).

Mineralization of spiramycin was investigated by measuring the organic carbon and the inorganic ions evolution as a function of the irradiation time (see Figure 2b). Under direct photolysis process, the carbon mineralization pursued a double kinetic. A pseudo first-order decay was followed within 16 h of irradiation and leaded to the abatement of 45 % of the initial organic carbon, while for longer irradiation time the mineralization slower proceeded; within 168 h of irradiation, only 58% of the organic carbon was mineralized. Conversely, the release of nitrogen from the molecule was only partially realized, with the formation of ammonium ions at 25% of the stoichiometric amount.

Under photocatalytic process, the complete carbon and nitrogen mineralization was obtained within 8h of irradiation. Nitrogen was mainly transformed into ammonium ions (85%) and in a minor extent into nitrate ions (15%). These results are in agreement with literature data, as it is known that tertiary and quaternary amino groups are mainly transformed into ammonium ions [30].

3.2. Transformation Products

The formation of intermediate compounds was monitored by HPLC/MS, which allowed following the initial fate of the drug. The TPs structural attributions were done by taking into account their chromatographic behavior and kinetics of evolution, coupled with accurate mass information, analysis of MS and MS^n spectra and comparison with parent drug fragmentation pathways. Their empirical formula was deduced from accurate mass values since, for all the unknown compounds, only one sum formula exists within a small mill-mass range (< 2 ppm), while the product ions formed in MSQ at high voltage or in LTQ-Orbitrap MS^2 and MS^3 spectra supported the structural attributions.

Approximate quantitation was done on the basis of spiramycin peak areas calibration curve. LOD and LOQ for this signal were respectively 9.0 and 31.0 μg L^{-1}.

3.2.1. Homogeneous Solution

While in dark experiments no transformation products were detected, upon irradiation the transformation of spiramycin proceeded through the formation of several TPs. Their amounts as a function of the irradiation time are plotted in Figure 3, while their MS product ions are summarized in Table 1. The proposed structures are collected in Scheme 2.

The organic compound with $[M+H]^+$ 526.3386 (labelled **B**) and empirical formula $C_{28}H_{48}NO_8$ could be formed through the detachment of mycaminose - mycarose sugar. The proposed structure was supported by MS^2 and MS^3 spectra analysis. MS^2 spectrum (see figure 4) showed a base peak at *m/z* 349.1933 (concerted loss of forosamine and water) and an intense ion at *m/z* 508.2873 (loss of a water molecule), compatible with the proposed structure shown in Scheme 2. The other product ions were formed from through the elimination of water and/or methanol from the lactone ring. The contemporaneous formation of a transformation product at $[M+H]^+$ 336.1937 (labelled **C**) was attributed to the mycarose/mycaminose sugar. **C** eliminates a mycarose molecule ($C_7H_{12}O_3$) with the formation of a product ion at *m/z* 192.1183, so bearing out the formation of the disaccharide. **B** and **C** contemporaneous formation suggested the cleavage of a C-O bond and the occurrence of a photo-assisted hydrolysis (see Scheme 2).

Looking closer to **D,** at *m/z* 702.4036 and empirical formula $C_{35}H_{60}NO_{13}$, its formation could involve the detachment of a forosamine molecule. A help in the structural attribution came from a

comparison between its product ions and those formed by spiramycin. Spiramycin produced the ions at *m/z* 699.4407 (loss of mycarose) and *m/z* 540.3147 (combined elimination of mycarose and forosamine). Analogously, **D** eliminated mycarose, with the formation of a product ion at *m/z* 540.3131, but not forosamine, in agreement with its detachment. A TP at *m/z* 160.1323 and empirical formula $C_8H_{18}NO_2$ was contemporaneously formed and attributed to hydroxyl-forosamine (**E**).

Their further transformation leads to the formation of a smaller molecule at *m/z* 176.1273 (**F**) and empirical formula $C_8H_{18}NO_3$, attributed to the protonated mycaminose, formed from the disaccharide transformation. The formation of another small molecule at *m/z* 144 (G) occurred. Unfortunately, this compound was only detected by MSQ;. The available information (at high cone voltage it lose a water molecule) did not permit to do a structural attribution. However, this species could be reasonably attributed to forosamine.

Taking into account the intermediates temporal profiles, it can be proposed that under illumination two initial transformation pathways occurred (see Scheme 2). The first transformation pathway (I) leads to the formation of two TPs with M.W. 525 and 335. A second photo-induced pathway (II) leads to the formation of the TPs **D** (M.W. 701) and **E** (M.W. 159), accordingly to a photo-assisted hydrolysis. Their further transformation leads to the formation of some smaller molecules at M.W. 175 (**F**), 143 (**G**) and 159 (**E**); **G** was reasonably formed from **B** degradation, while the formation of the other two species cannot be attributed to a specific transformation pathway.

3.2.2. Heterogeneous Photocatalysis

In the photocatalytic experiment, numerous TPs were formed, whose profiles as a function of the irradiation time are plotted in Figure 5. All the TPs identified by direct photolysis process were still formed and reached their maxima amounts until 15 min of irradiation. In addition, some new intermediate compounds, labelled **H** ($[M+H]^+$ 699.4404) and **I** ($[M+H]^+$ 859.5153) were formed and starts some additional pathways (see pathways III and IV in scheme 2).

H shared the same empirical formula and MS^n product ions with an MS^2 spiramycin product ion and was attributed to neospiramycin. Injection of a neospiramycin standard solution confirmed this structural attribution. It has to be underlined that, even if spiramycin is known to be converted in neospiramycin at acidic conditions (pH < 2) [31] in our experimental conditions (pH 6.2) its conversion into neospiramycin is negligible; therefore, the observed formation of neospiramycin

was induced by the photocatalytic process. Its formation rapidly occurs (highest amount is reached after 5 min of irradiation) and easily disappears until 15 min.

A fourth transformation pathway (IV) leads to the spiramycin hydroxylation, with the formation of the intermediate compound **I** ($[M+H]^+$ 859.5153). Unfortunately, the available MS information did not permit to allocate the OH group, but only to exclude the involvement of forosamine (see *m/z* 715.4375, loss of forosamine) and mycarose moieties (see *m/z* 556.3116, combined elimination of mycarose and forosamine).

3.3. Transformation of Spiramycin in River Water

3.3.1. Laboratory Simulation

Po river water was sampled in Turin on 04 July 2008, spiked with spiramycin (15 mg L^{-1}) and analysed. Dark experiments showed that the disappearance of spiramycin slowly occurred (see Figure 2) and in the considered times (10 days) no TPs were formed at a detectable concentration. Under illumination its transformation occurred ($t_{1/2}$ passes from 260 to 25 h) and proceeded through the formation of the TPs plotted in Figure 6. Most of them coincide with those formed through a photo-induced process (see structures labelled **B**, **C**, **E**, **F**, **H** and **I**). The TPs **B**, **C**, **E** and **F** were formed in homogeneous solution under irradiation (see figure 3), so that their formation could be attributed to a direct photolysis process. Conversely, the formation of **H** and **I** seems due to indirect photo-induced processes, mediated by natural photo sensitizers.

In addition, three new TPs were identified and start a fifth transformation route. Two structural isomers with $[M+H]^+$ 829.5053, labelled **J** and **K**, were formed through a demethylation reaction (see Table 1 and Scheme 2). By analysing their MS product ions, **J** gave the product ions at (1) *m/z* 685.4270, attributed to the mycarose loss, (2) *m/z* 526.3413, produced through the elimination of mycarose/demethylated mycaminose) and (3) m/z 670.3806, formed from forosamine and mycarose detachment. Hence, the methyl group was reasonably lost from the mycaminose moiety. **K** showed a product ion at *m/z* 702.4034, well-matched with the loss of the demethylated forosamine.

The formation of **L** (*m/z* 815.4910) involved the detachment of two methyl groups. The presence of a product ion at *m/z* 671.4123 excluded a demethylation of mycarose, while the product ion at *m/z* 540.3138 suggested the detachment of both methyl groups from the forosamine moiety. The TPs evolution as a function of the irradiation time suggests that **L** was formed through **K** demethylation.

3.3.2. In Field Transformations

A preliminary sampling campaign was performed from 1 to 4 July 2008 along the whole Po river tract. The map showing the sampling points is reported in the figure S1, while their chemical-physic features are listed in Table S1. The samples were concentrated on SPE cartridge (see section 2.4) and analyzed by HPLC/HRMS. Spiramycin and its transformation products were searched in all samples (see Table 2).

Sample 1 was collected close to the river source and neither the spiramycin nor its transformation products were detected. Spiramycin was found in the sample 2 (Moncalieri, before Turin) and in the sample 7 (Pontelagoscuro di Ferrara) at a concentration of 1.82 ngL^{-1} and 29.8 ng/L, respectively. These concentrations are in agreement with literature studies [16-18].

Looking closer to the identified TPs, in samples 2 and 7 were detected **I** (*m/z* 859.5153, hydroxyspiramycin) and **K** (*m/z* 829.5053 demethylated spiramycin), while **H** (*m/z* 699.4406, neospiramycin) was identified in sample 7 only. It is worth noting that these three compounds coincide with the TPs formed at a higher rate (and amount) in the laboratory experiments performed on river water spiked with spiramycin. Furthermore, **I** and **H** were also formed during photocatalytic experiments, but not for direct photolysis (see Figure 3), so that their formation in the Po River samples could be attributed to indirect photolysis processes mediated by natural species such as dissolved organic matter, nitrite and nitrate ions, H_2O_2 and iron species [32].

B (*m/z* 526.3386, formed through the detachment of mycarose – mycaminose) was found in samples 3 (Turin), 4 (San Raffaele Cimena (after Turin)), 5 (Spessa (Pavia)), 6 (Casalmaggiore (Cremona)) and 8 (Porto Tolle (Rovigo)), while **D** (*m/z* 702, detachment of forosamine) was formed in sample 5 only. Both the TPs were identified during the photolysis experiments. Their presence was noted in samples taken downstream to not-transformed spiramycin and it could be due to their slower formation rate. Owing to the spiramycin disappearance rate and the TPs evolution profiles measured in Po river water (see Figure 6), it can be proposed a spiramycin source located not far from points 2 and 7. Spiramycin was then rapidly transformed, so that only the more persistent TPs can be found downstream. The high amount of the transformation products **B** and **D** in sample 5 could be justified by the presence of a spiramycin source located between 4 and 5, so far to permit the drug degradation, but not the TPs disappearance. The formation of **D** in the same sample, formed slower than **I** and **H**, supports the proposed source.

3.4. Toxicity Assessment

Ecotoxicological effect in the aquatic ecosystem was evaluated by using the *Vibrio Fischeri* luminescent bacteria assay, a test appropriate for aquatic samples and that showed a good correlation with other bioassays [32]. The toxicity of spiramycin in sterilized or river water collected at different irradiation times was examined and plotted in Figure 7. The initial toxicity of pure spiramycin (0 h of irradiation) showed an inhibition of 0% (no toxic compounds). For the samples irradiated at different times, the toxicity increases in all cases, due to the formation of toxic TPs. By analysing the toxicity curve in sterilized water added with TiO_2 (Figure 7, top), after 15 min of irradiation the percentage of inhibition was highest (30 %) and then decreases until 4h of irradiation (no toxicity). When comparing the toxicity curve with the TPs temporal profiles, it can be noted that at 15 min the concentration of **G**, **E** and **F** was maxima. Hence, the measured toxicity could be linked to these intermediate compounds, while **B**, **H** and **I** did not contribute.

Opposite to the photocatalytic samples, the toxicity curve measured in pure water showed a continuous increasing in the inhibition percentage for the considered time (see Figure 7, bottom). Since none of the identified compounds follows a similar profile, the measured toxicity cannot be correlated with the identified TPs. However, among the recognized intermediates, **E** and **F** might contribute to the measured toxicity.

Analogously, the toxicity measured in the Po River samples cannot be attributed to a specific compound; nevertheless, the TPs temporal profiles allowed to exclude a possible contribute by **K**, **J**, **B**, **L** and **H**. We can then conclude that four of the TPs identified in the Po river samples are non toxic compounds, while for **D** a possible toxic effect cannot be excluded.

Conclusions

The photocatalytic model demonstrated itself helpful to identify a number of degradation compounds, whose measurement gives a useful tool to monitor drug presence and transformation in environmental analysis. A preliminary screening of the Po River across its whole tract has permitted to evidence the existence of some peculiar zones, characterized by strong source or dilution. Within this contest, the study of the environmental fate of the selected drug was done. The drug had a short residence time, but its transformation proceeded through the formation of more persistent compounds. Even if the drug presence was detected only in few river points, its transformation products were found in more samples and, in some cases, at so high amounts to be only justified by assuming a higher number of source points than those attributable on the basis of the drug

monitoring. In the future this approach will be applied in a more systematic way, in order to characterize the quantitative variation of each compound in aquatic system.

Literature Cited

[1] Zwiener, C.; (2007) Occurrence and analysis of pharmaceuticals and their transformation products in drinking water treatment, Anal. Bioanal. Chem. 387, 1159–1162

[2] Khetan, S.K. and Collins, T.J. (2007) Human Pharmaceuticals in the Aquatic Environment: A Challenge to Green Chemistry. Chem. Rev. 107, 2319-2364.

[3] Barceló, D.; Petrovic, M. (2007) Pharmaceuticals and personal care products (PPCPs) in the environment Anal. Bioanal. Chem .387, 1141–1142

[4] Ellis, J.B. (2006) Pharmaceutical and personal care products (PPCPs) in urban receiving waters, Environ. Pollution 144 (1), 184-189

[5] Heberer, T. (2002) Occurrence, fate, and removal of pharmaceutical residues in the aquatic environment: a review of recent research data. Toxicol. Lett. 131, 5-17

[6] Costanzo, S.D.; Murby, J. and Bates J. (2005) Ecosystem response to antibiotics entering the aquatic environment, Mar. Pollut. Bull. 51(1-4), 218-223

[7] Hao, C.; Zhao, X. and Yang, P. (2007) GC-MS and HPLC-MS analysis of bioactive pharmaceuticals and personal-care products in environmental matrices TrAC Trends in Anal. Chem. 26(6), 569-580

[8] Rang, H.P.; Dale, M.M. and Ritter, J.M. (2003) Pharmacology (4th edition)" Churchill Livingstone, Edinburgh

[9] Abu-Gharbieh, E.; Vasina, V.; Poluzzi, E. and De Ponti F. (2004) Antibacterial macrolides: a drug class with a complex pharmacological profile. Pharm. Res. 50 (3), 211-222

[10] Collignon, P. (1999) Vancomycin-resistant enterococci and use of avoparcin in animal feed: is there a link? Med. J. Australia 171, 144–146

[11] González de la Huebra, M.J.; Vincent, U.; Bordin, G. and Rodrıguez, A.R. (2004) Characterisation of dirithromycin and spiramycin using high performance liquid chromatography and direct infusion mass spectrometry" Anal. Chim. Acta 503 (2), 247-256

[12] Sagan, C.; Salvador, A.; Dubreuil, D.; Poulet, P.P.; Duffault, D. and Brumpt, I. (2005) Simultaneous determination of metronidazole and spiramycin I in human plasma, saliva and gingival crevicular fluid by LC-MS/MS. J. Pharmac. Biomed. Anal., 38, 298-306

[13] Dubois, M.; Fluchard, D.; Sior, E. and Delahaut, P. (2001) Identification and quantification of five macrolide antibiotics in several tissues, eggs and milk by liquid chromatography-electrospray tandem mass spectrometry J. Chromat. B 753, 189-202

[14] Zhengqi, Y. and Weinberg, H.S. (2007) Trace Analysis of Trimethoprim and Sulfonamide, Macrolide, Quinolone, and Tetracycline Antibiotics in Chlorinated Drinking Water Using Liquid Chromatography Electrospray Tandem Mass Spectrometry, Anal. Chem. 79 (3), 1135-1144

[15] Kees, F.; Spangler, S. and Wellenhofer, M. (1998) Determination of macrolides in biological matrices by high-performance liquid chromatography with electrochemical detection. J. Chromatogr. A 812 (1-2), 287-293

[16] Castiglioni, S.; Fanelli, R.; Calamari, D.; Bagnati, R. and Zuccato, E. (2004) Methodological approaches for studying pharmaceuticals in the environment by comparing predicted and measured concentrations in River Po, Italy. Regul. Toxicol. Pharmacol. 39 (1), 25-32

[17] Zuccato, E.; Castiglioni, S.; Fanelli, R.; Reitano, G.; Bagnati, R.; Chiabrando, C.; Pomati, F.;. Rossetti, C.; Calamari, D. (2006) Pharmaceutical in the environment in Italy: causes, occurrence, effects and control Environ. Sci. Pollut. Res. 13 (1), 15-21

[18] Zuccato, E., Calamari, D.; Natangelo, M.; Fanelli, R. (2000) Presence of therapeutic drugs in the environment, Lancet 355 (9217), 1789-1790

[19] Richardson, M.A.; Kuhstoss, S.; Huber, M.L.B.; Ford, L.; Godfrey, O.; Turner, J.R. and Nagaraja Rao, R. (1990) Cloning of Spiramycin Biosynthetic Genes and Their Use in Constructing Streptomyces ambofaciens Mutants Defective in Spiramycin Biosynthesis, J. Bacteriol. 172 (7), 3790-3798

[20] Ikeda, O.S.; Kitao, H. (1979) Isolation and properties of Spiramycin I 3-hydroxil acylase from Streptomyces ambofaciens, J. Biochem., 86, 1753-1758

[21] Cherlet, M.; De Baere, S.; Croubels, S. and De Backer, P. (2002) Quantitation of tylosin in swine tissues by liquid chromatography combined with electrospray ionization mass spectrometry. Anal. Chim. Acta 473 (1-2), 167-175

[22] Mourier, P. and Brun, A. (1997) Study of the metabolism of spiramycin in pig liver. J. Chromatography B 704, 197-205

[23] Sakkas, V.A.; Calza, P.; Medana, C.; Villioti, A.E.; Baiocchi, C.; Pelizzetti, E.; Albanis, T. (2007) Heterogeneous photocatalytic degradation of the pharmaceutical agent salbutamol in aqueous titanium dioxide suspensions. Appl. Catal. B: Environ. 77, 135-144

[24] Molinari, R.; Pirillo, F.; Loddo, V. and Palmisano, L. (2006) Heterogeneous photocatalytic degradation of pharmaceuticals in water by using polycrystalline TiO_2 and a nanofiltration membrane reactor. Catal. Today 118, 205-213

[25] Doll, T.E. and Frimmel, F.H. (2005) Removal of selected persistent organic pollutants by heterogeneous photocatalysis in water Catal. Today 101, 195-202

[26] Calza, P.; Sakkas, V.A.; Medana, C., Baiocchi, C.; Dimou, A.; Pelizzetti, E. and Albanis, T. (2006) Photocatalytic degradation study of diclofenac over aqueous TiO_2 suspensions Appl. Catal. B: Environ. 67, 197

[27] Zwiener, C. and Frimmel, F.H. (2000) Oxidative treatment of pharmaceuticals in water Water Res., 34, 1881-1885

[28] Calza, P.; Medana, C.; Pazzi, M.; Baiocchi, C.; Pelizzetti. E. (2004) The photocatalytic process as a tool to identify metabolitic products formed from dopant substances: the case of buspirone. J. Pharm Biomed. Anal. 35, 9-19

[29] Marsh, J.R.; Weiss, P.J. (1967) Solubility of antibiotics in twenty-six solvents. III. J. A.O.A.C. 50, 457-462.

[30] Nohara, K.; Hidaka, H.; Pelizzetti, E.; Serpone, N. (1997) Processes of formation of NH_4^+ and NO_3^- ions during the photocatalyzed oxidation of N-containing compounds at the titania/water interface. J. Photochem. Photobiol. A Chem. 102 (2-3), 265-272

[31] Ramu, K.; Shringarpure, S. and Williamson, J.S. (1995) A solution conformation analysis of forocidins-I and isoforocidins-I using NMR and molecular modeling. Pharm. Res. 12, 621-629

[32] Boule, P.; Bahenmann, DW.; Robertson, DW. and Robertson, P.K.J. (2005) The handbook of environmental Chemistry, Springer ed., Berlin.

[33] Parvez S., Venkataraman C., Mukherji S., A review on advantages of implementing luminescence inhibition test (Vibrio fischeri) for acute toxicity prediction of chemicals, Environ. Int., 2006; 32:265-268.

STRUCTURE	$[M+H]^+$	t_R (min.)	MSQ		LTQ-Orbitrap	
			Cone voltage	Product ions	MS^2	MS^3

Table 1. Intermediate compounds formed from spiramycin transformation and detected by HPLC/MS: (a) under direct photolysis in sterilized water; (b) upon photocatalytic process; (c) upon illumination in Po river water. In square brackets are reported the ion relative intensities.

A	843.5210	11.85	50	699 (-$C_7H_{12}O_3$ [10]) 540(-$C_7H_{12}O_3$,-$C_8H_{17}NO_2$ [30])	699.4407 [14]	540.3147 [100] 558.3132 [30] 522.3043 [25] 681.4326 [20]
					684.3934 [20]	540.3147 [100]
					540.3147 [34]	522.3043 [75] 349.1923 [22] 174.1081 [100]
					522.3043 [11]	490.2675 [100] 207.0039 [25]
			90	540(-$C_7H_{12}O_3$,-$C_8H_{17}NO_2$ [70])		
B (a, b, c)	526.3386	12.46	50	-	349.1933 [100]	299.1575 [100] 331.1831 [37]
					508.2873 [90]	490.2674 [100]
					331.1891 [44]	-
					317.1736 [46]	-
					299.1631 [54]	-
C (a, b)	336.1937	2.85	50	192 (-$C_7H_{12}O_3$ [50])	192.1183 [100]	-
			70	192 (-$C_7H_{12}O_3$ [100])	174.1082 [28]	-
			90	192 (-$C_7H_{12}O_3$ [100]) 174 (-H_2O, -$C_7H_{12}O_3$ [100])		
D (a,c)	702.4036	12.60	50	-	540.3131 [24]	-
			70	540 (-$C_7H_{12}O_4$[50])	558.3237 [100]	-
			90	-		
E (a, b, c)	160.1323	2.51	50:	_	142.1217 [100]	-
			70	142 (-H_2O [18])		
			90	142 (-H_2O [65])		
F (a, b, c)	176.1273	2.15	50	158 (-H_2O [20])	158.1166 [100]	140.0669 [100] 112.0725 [40]
			70	158 (-H_2O [86])		
			90	158 (-H_2O [100])		
G (a, b)	144	2.21	50	-	-	
			70	-		
			90	126 (-H_2O [100])		
H (b, c)	699.4404	10.32	50	542(-$C_8H_{15}NO_2$ [40])	522.3035 [44]	490 [100] 174 [20]
					540.3138 [100]	522.2933 [40] 349.1931 [10] 174.1082 [100]
I (b, c)	859.5153	9.38	50	-	715.4375 [100]	-
					556.3116 [30]	-
J (c)	829.5053	10.50	50	685 (-$C_7H_{12}O_3$ [27]) 526(-$C_7H_{12}O_3$,-$C_8H_{17}NO_2$ [45])	685.4270 [35]	540.3131 [100]
					670.3806 [100]	-
					526.3413 [70]	-
K (c)		11.45	50	702 (-$C_7H_{13}NO$ [100])	702.4034 [100]	-
L(c)	815.4910	10.20	50	688 (-$C_7H_{13}NO$ [100]) 671 (-$C_7H_{12}O_3$ [55])	671.4123 [100]	-
					540.3138 [82]	-

Table 2. Spiramycin and its transformation products in Po river samples. In round brackets is reported the concentration of spiramycin.

	Area (x10^5)					
	Spiramycin	**I (*m/z* 859.5153)**	**K (*m/z* 829.5053)**	**H (*m/z* 699.4407)**	**D (*m/z* 702.4034)**	**B (*m/z* 526.2986)**
Sample 1	-	-	-	-	-	-
Sample 2	0.66 (1.82 ng L^{-1})	0.20	0.26	-	-	-
Sample 3	-	-	-	-	-	0.46
Sample 4	-	-	-	-	-	0.20
Sample 5	-	-	-	-	0.84	1.47
Sample 6	-	-	-	-	-	0.16
Sample 7	10.8 (29.8 ng L^{-1})	0.76	2.17	0.43	-	-
Sample 8	-	-	-	-	-	0.20

Figure captions

Figure 1. Structure of spiramycin.

Figure 2. Degradation of spiramycin 15 mg L^{-1} as a function of the irradiation time in sterilized water, river water or sterilized water added with TiO_2 (100 mg L^{-1}) (a) disappearance of initial compound in river water and sterilized water and, in inset in TiO_2 suspension and (b) TOC disappearance, nitrate and ammonium evolution as a function of the irradiation time.

Figure 3. Intermediates generated from spiramycin degradation in sterilized water as a function of the irradiation time under direct photolysis.

Figure 4. MS^2 spectra for the species at m/z 526.2986.

Figure 5. Intermediates formed from spiramycin degradation in sterilized water added with TiO_2 as a function of the irradiation time under photocatalytic process.

Figure 6. Intermediates generated from spiramycin degradation as a function of the irradiation time in Po river water.

Figure 7. Inhibition (%) of the luminescence of bacteria *Vibrio fischeri* as a function of the treatment time for spiramycin; (top) under photocatalytic treatment and (bottom) sterilized or river water spiked with 15 mg L^{-1} of spiramycin.

Scheme 1. Fragmentation pathways followed by spiramycin.

Scheme 2. Possible initial transformation photo-induced pathways followed by spiramycin.

Figure1

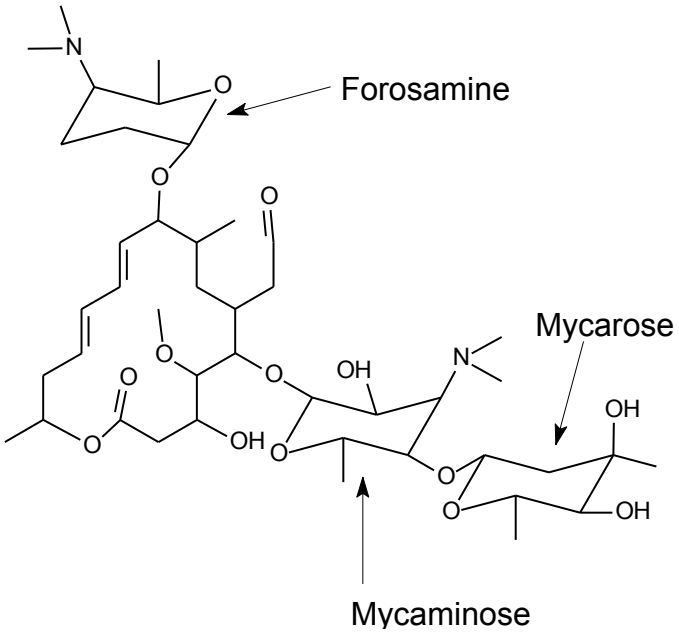

Figure 2

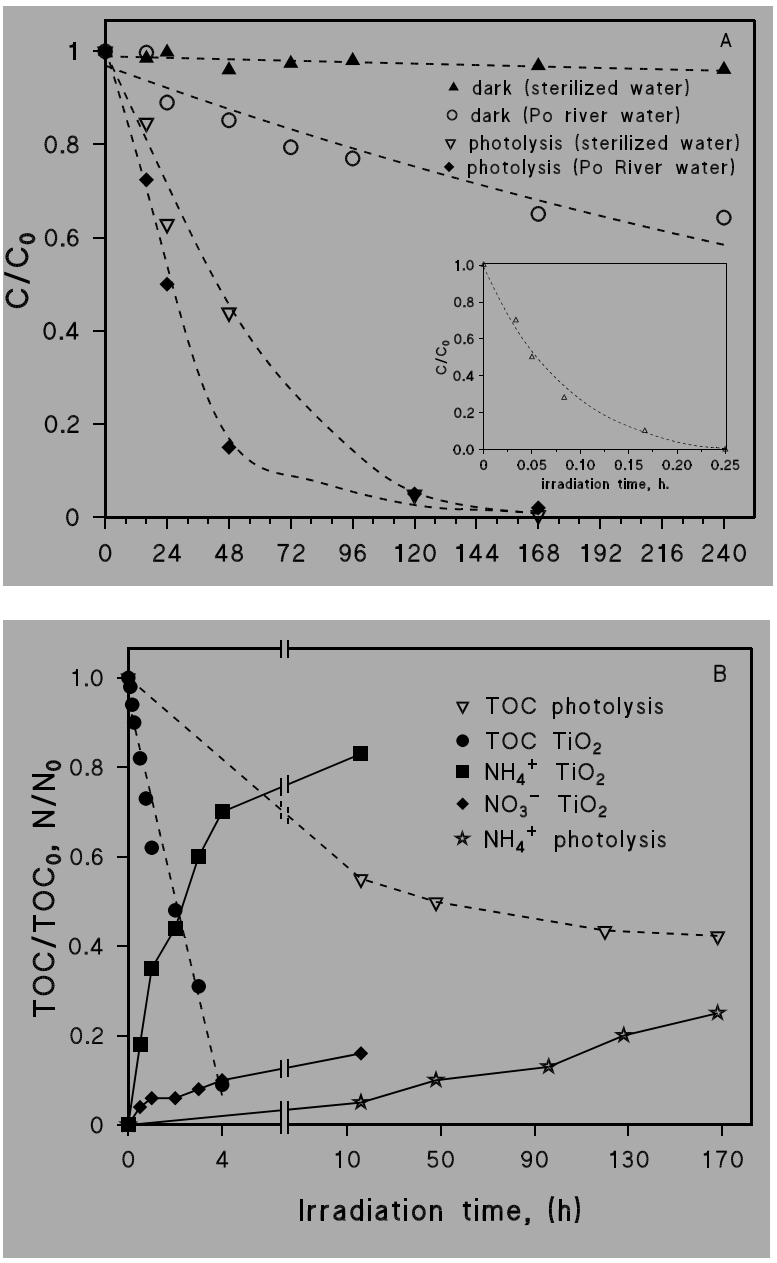
A
dark (sterilized water)
dark (Po river water)
photolysis (sterilized water)
photolysis (Po River water)
C/C0
irradiation time, h.
B
TOC photolysis
TOC TiO2
NH4+ TiO2
NO3− TiO2
NH4+ photolysis
TOC/TOC0, N/N0
Irradiation time, (h)

Figure 3

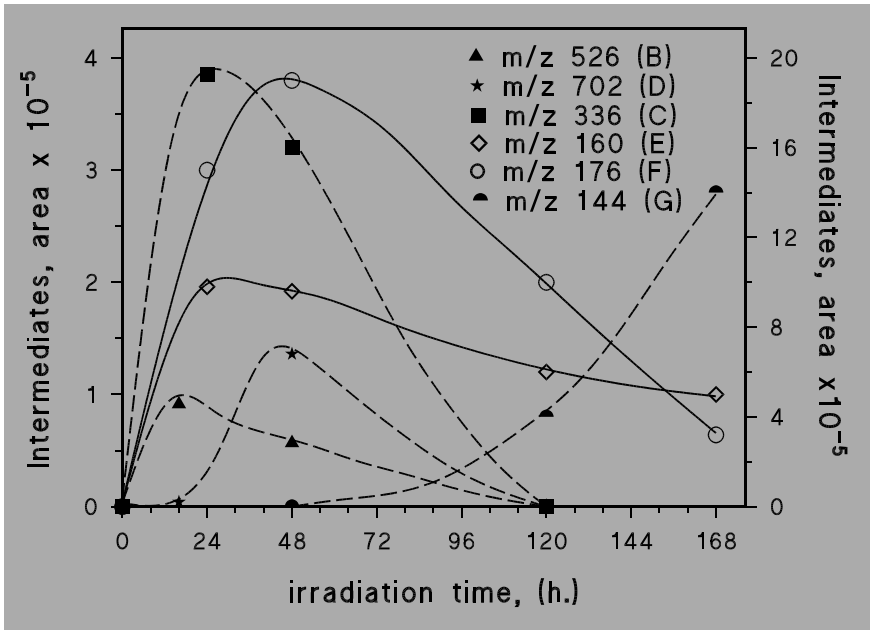
m/z 526 (B)
m/z 702 (D)
m/z 336 (C)
m/z 160 (E)
m/z 176 (F)
m/z 144 (G)
Intermediates, area x 10⁻⁵
Intermediates, area x10⁻⁵
irradiation time, (h.)
0
24
48
72
96
120
144
168
1
2
3
4
8
12
16
20

Figure 4

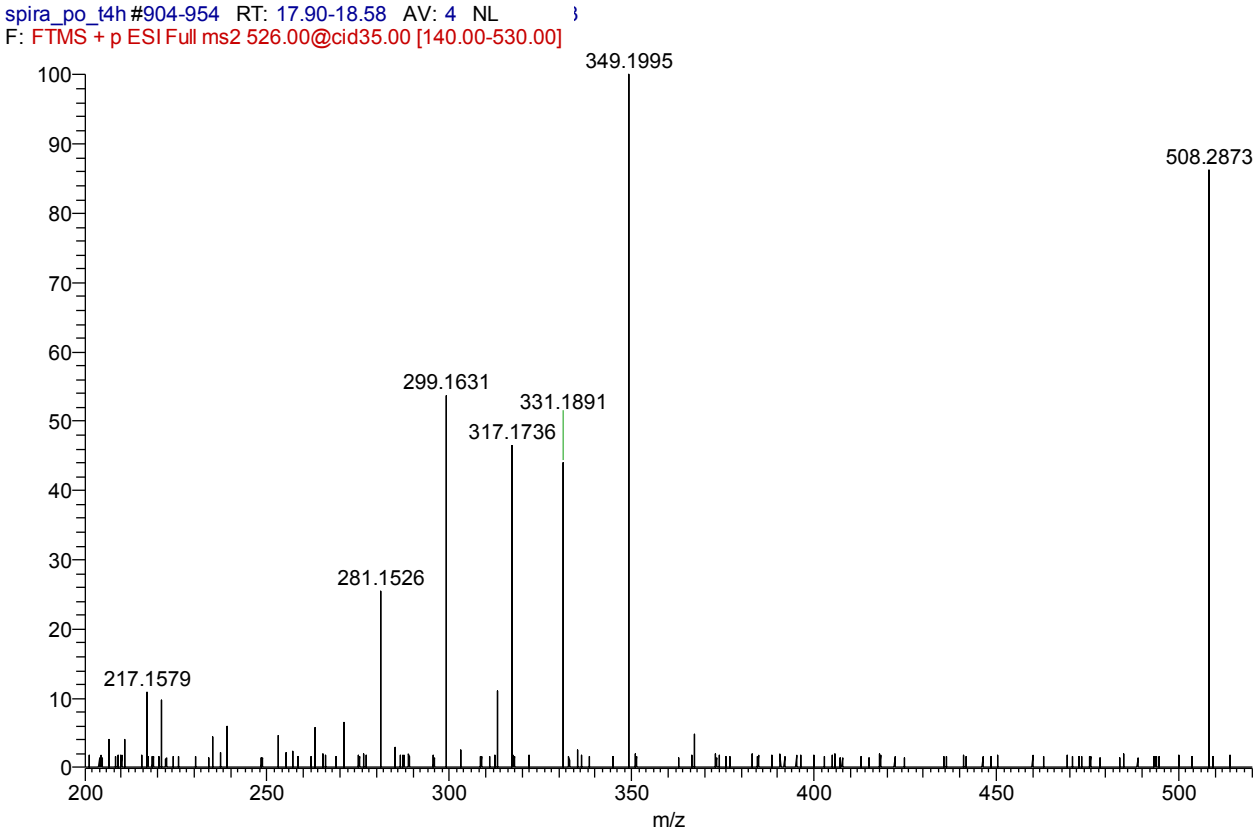
spira_po_t4h #904-954 RT: 17.90-18.58 AV: 4 NL
F: FTMS + p ESI Full ms2 526.00@cid35.00 [140.00-530.00]
349.1995
508.2873
299.1631
331.1891
317.1736
281.1526
217.1579
100
90
80
70
60
50
40
30
20
10
0
200
250
300
350
400
450
500
m/z

Figure 5

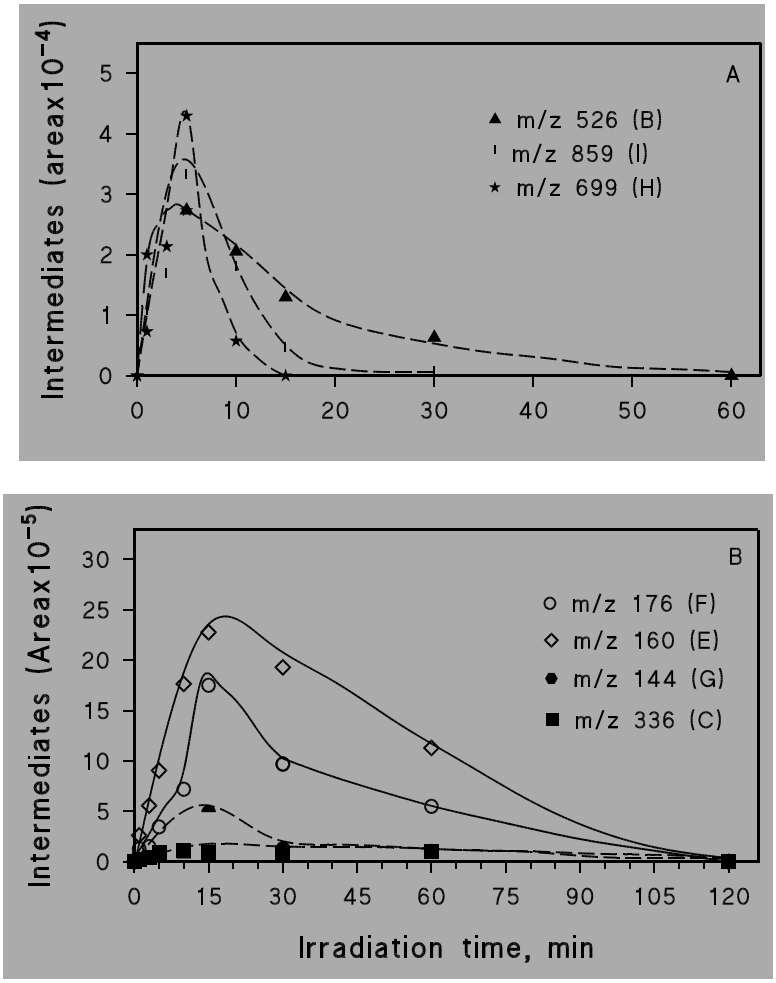
A
m/z 526 (B)
m/z 859 (I)
m/z 699 (H)
Intermediates (areax10⁻⁴)
0
1
2
3
4
5
0
10
20
30
40
50
60
B
m/z 176 (F)
m/z 160 (E)
m/z 144 (G)
m/z 336 (C)
Intermediates (Areax10⁻⁵)
0
5
10
15
20
25
30
0
15
30
45
60
75
90
105
120
Irradiation time, min

Figure 6

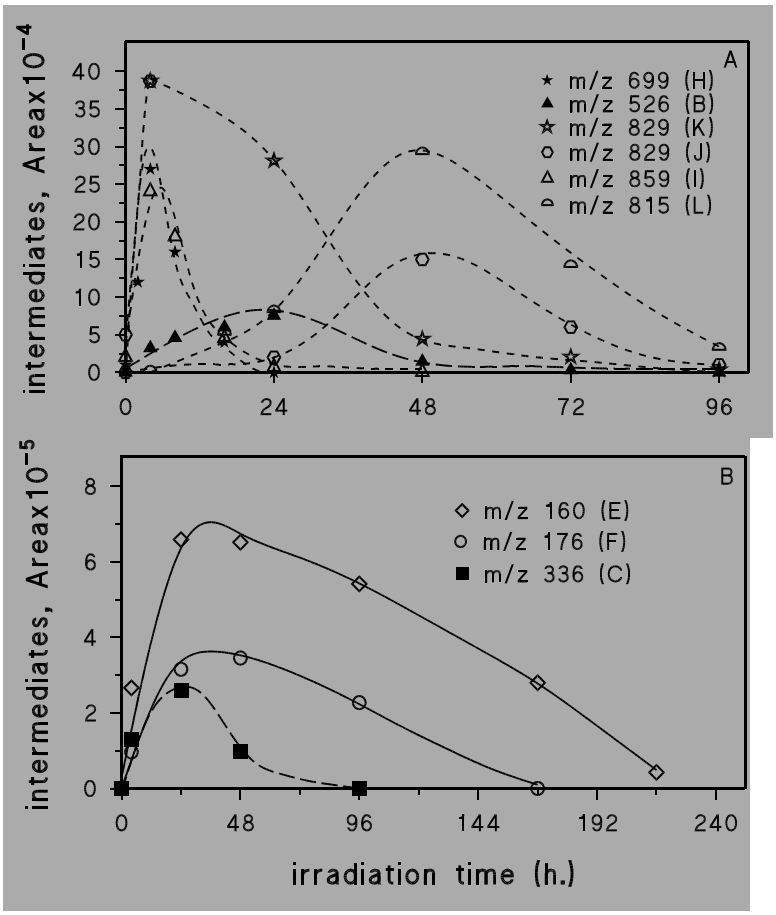
A
m/z 699 (H)
m/z 526 (B)
m/z 829 (K)
m/z 829 (J)
m/z 859 (I)
m/z 815 (L)
intermediates, Areax10⁻⁴
0
5
10
15
20
25
30
35
40
0
24
48
72
96
B
m/z 160 (E)
m/z 176 (F)
m/z 336 (C)
intermediates, Areax10⁻⁵
0
2
4
6
8
0
48
96
144
192
240
irradiation time (h.)

Figure 7

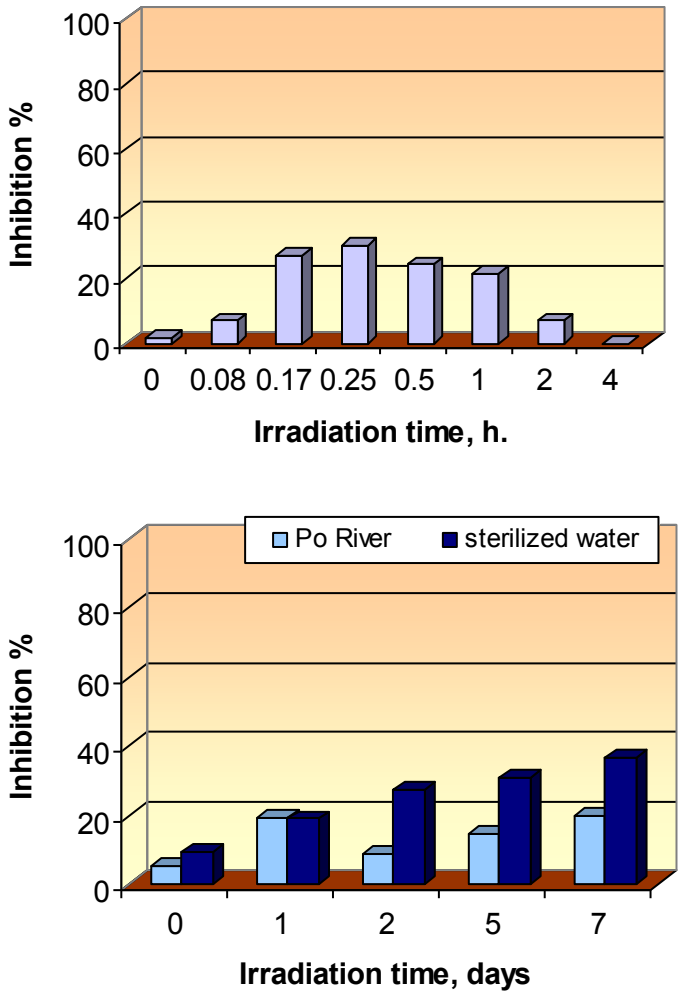
100
80
60
40
20
0
Inhibition %
0
0.08
0.17
0.25
0.5
1
2
4
Irradiation time, h.
Po River
sterilized water
100
80
60
40
20
0
Inhibition %
0
1
2
5
7
Irradiation time, days

SCHEME 1

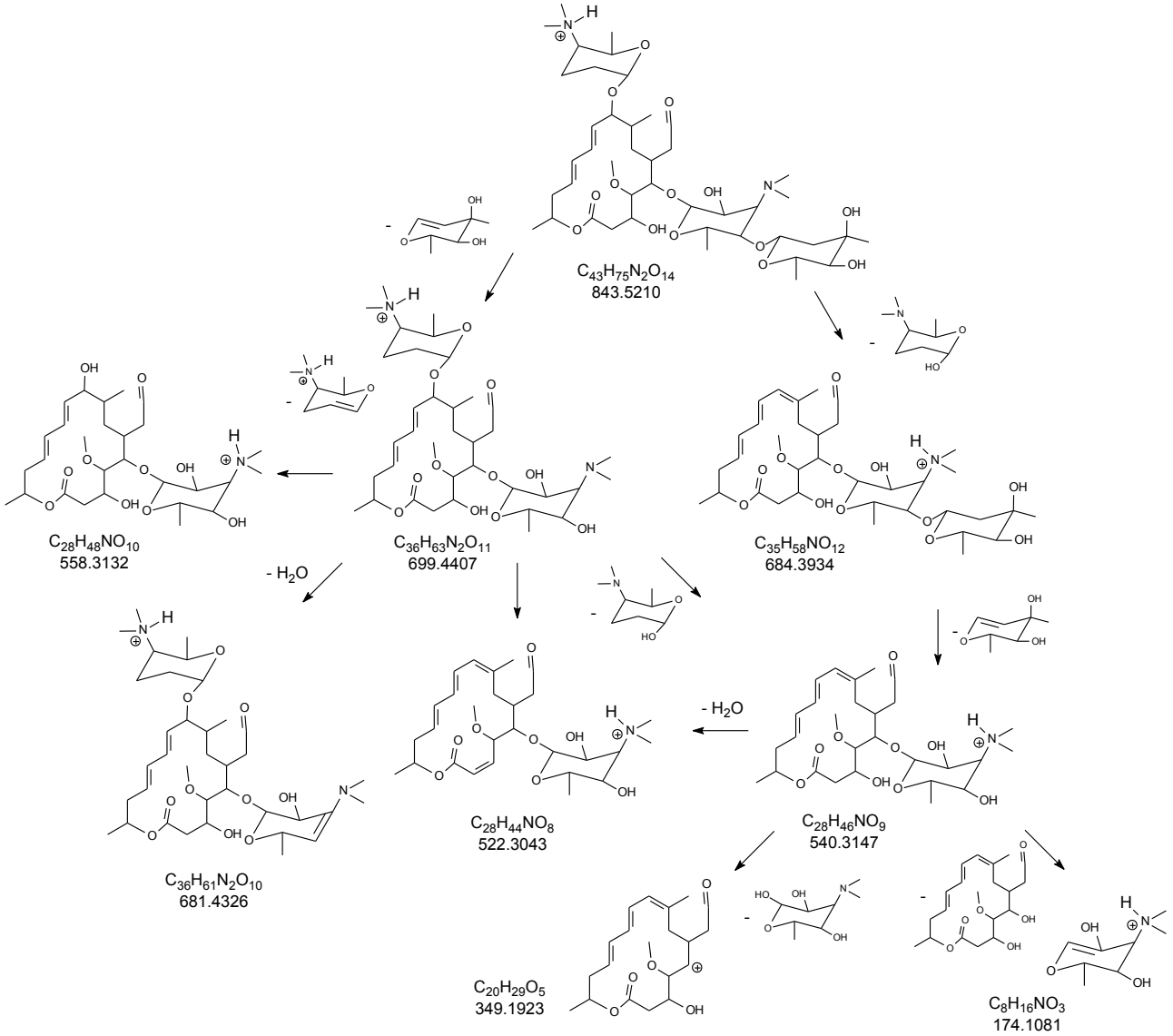
C43H75N2O14
843.5210
C28H48NO10
558.3132
C36H63N2O11
699.4407
C35H58NO12
684.3934
- H2O
C36H61N2O10
681.4326
C28H44NO8
522.3043
- H2O
C28H46NO9
540.3147
C20H29O5
349.1923
C8H16NO3
174.1081

SCHEME 2

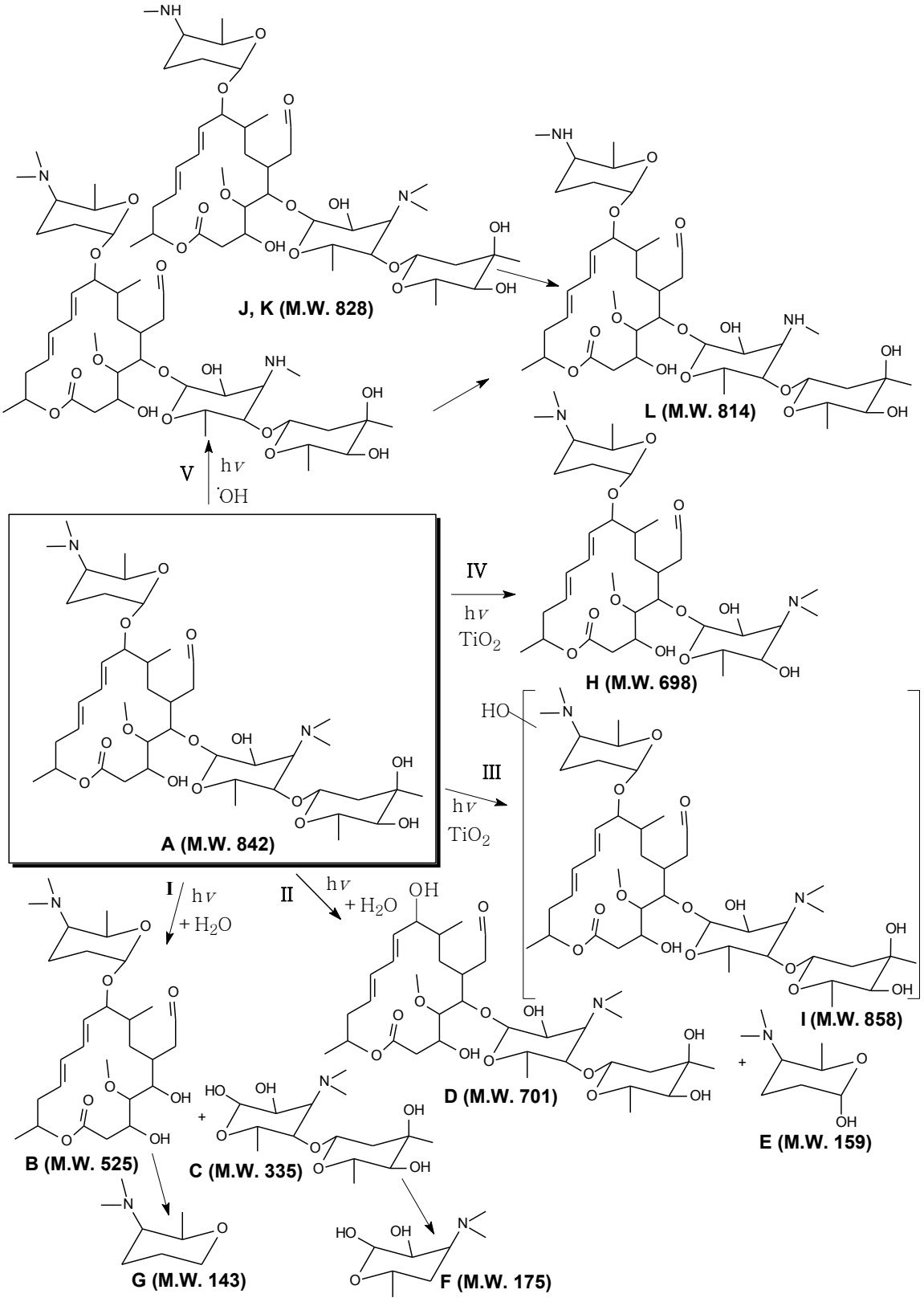
J, K (M.W. 828)
L (M.W. 814)
V
hν
·OH
IV
hν
TiO2
H (M.W. 698)
A (M.W. 842)
III
hν
TiO2
I (M.W. 858)
I
hν
+ H2O
II
hν
+ H2O
D (M.W. 701)
E (M.W. 159)
B (M.W. 525)
C (M.W. 335)
G (M.W. 143)
F (M.W. 175)